JOURNAL OF Applied Polymer SCIENCE

Special Issue: Bio-based Packaging

Guest Editors: José M. Lagarón, Amparo López-Rubio, and María José Fabra
Institute of Agrochemistry and Food Technology of the Spanish Council for Scientific Research

EDITORIAL

REVIEWS

RESEARCH ARTICLES

JOURNAL OF Applied Polymer SCIENCE

Special Issue: Bio-based Packaging

Guest Editors: José M. Lagarón, Amparo López-Rubio, and María José Fabra
Institute of Agrochemistry and Food Technology of the Spanish Council for Scientific Research

Impact of fermentation residues on the thermal, structural, and rheological properties of polyhydroxy(butyrate-*co*-valerate) produced from cheese whey and olive oil mill wastewater
L. Hilliou, D. Machado, C. S. S. Oliveira, A. R. Gouveia, M. A. M. Reis, S. Campanari, M. Villano and M. Majone, *J. Appl. Polym. Sci.* 2015, DOI: 10.1002/app.42818

Synergistic effect of lactic acid oligomers and laminar graphene sheets on the barrier properties of polylactide nanocomposites obtained by the in situ polymerization pre-incorporation method
J. Ambrosio-Martín, A. López-Rubio, M. J. Fabra, M. A. López-Manchado, A. Sorrentino, G. Gorrasi and J. M. Lagarón, *J. Appl. Polym. Sci.* 2015, DOI: 10.1002/app.42661

Antibacterial poly(lactic acid) (PLA) films grafted with electrospun PLA/allyl isothiocyanate fibers for food packaging
H. H. Kara, F. Xiao, M. Sarker, T. Z. Jin, A. M. M. Sousa, C.-K. Liu, P. M. Tomasula and L. Liu, *J. Appl. Polym. Sci.* 2015, DOI: 10.1002/app.42475

Poly(L-lactide)/ZnO nanocomposites as efficient UV-shielding coatings for packaging applications
E. Lizundia, L. Ruiz-Rubio, J. L. Vilas and L. M. León, *J. Appl. Polym. Sci.* 2015, DOI: 10.1002/app.42426

Effect of electron beam irradiation on the properties of polylactic acid/montmorillonite nanocomposites for food packaging applications
M. Salvatore, A. Marra, D. Duraccio, S. Shayanfar, S. D. Pillai, S. Cimmino and C. Silvestre, *J. Appl. Polym. Sci.* 2015, DOI: 10.1002/app.42219

Preparation and characterization of linear and star-shaped poly L-lactide blends
M. B. Khajeheian and A. Rosling, *J. Appl. Polym. Sci.* 2015, DOI: 10.1002/app.42231

Mechanical properties of biodegradable polylactide/poly(ether-block-amide)/thermoplastic starch blends: Effect of the crosslinking of starch
L. Zhou, G. Zhao and W. Jiang, *J. Appl. Polym. Sci.* 2015, DOI: 10.1002/app.42297

Interaction and quantification of thymol in active PLA-based materials containing natural fibers
I. S. M. A. Tawakkal, M. J. Cran and S. W. Bigger, *J. Appl. Polym. Sci.* 2015, DOI: 10.1002/app.42160

Graphene-modified poly(lactic acid) for packaging: Material formulation, processing, and performance
M. Barletta, M. Puopolo, V. Tagliaferri and S. Vesco, *J. Appl. Polym. Sci.* 2015, DOI: 10.1002/app.42252

Edible films based on chia flour: Development and characterization
M. Dick, C. H. Pagno, T. M. H. Costa, A. Gomaa, M. Subirade, A. De O. Rios and S. H. Flóres, *J. Appl. Polym. Sci.* 2015, DOI: 10.1002/app.42455

Influence of citric acid on the properties and stability of starch-polycaprolactone based films
R. Ortega-Toro, S. Collazo-Bigliardi, P. Talens and A. Chiralt, *J. Appl. Polym. Sci.* 2015, DOI: 10.1002/app.42220

Bionanocomposites based on polysaccharides and fibrous clays for packaging applications
A. C. S. Alcântara, M. Darder, P. Aranda, A. Ayral and E. Ruiz-Hitzky, *J. Appl. Polym. Sci.* 2015, DOI: 10.1002/app.42362

Hybrid carrageenan-based formulations for edible film preparation: Benchmarking with kappa carrageenan
F. D. S. Larotonda, M. D. Torres, M. P. Gonçalves, A. M. Sereno and L. Hilliou, *J. Appl. Polym. Sci.* 2015, DOI: 10.1002/app.42263

JOURNAL OF Applied Polymer SCIENCE

Special Issue: Bio-based Packaging

Guest Editors: José M. Lagarón, Amparo López-Rubio, and María José Fabra
Institute of Agrochemistry and Food Technology of the Spanish Council for Scientific Research

Structural and mechanical properties of clay nanocomposite foams based on cellulose for the food packaging industry
S. Ahmadzadeh, J. Keramat, A. Nasirpour, N. Hamdami, T. Behzad, L. Aranda, M. Vilasi and S. Desobry, *J. Appl. Polym. Sci.* 2015, DOI: 10.1002/app.42079

Mechanically strong nanocomposite films based on highly filled carboxymethyl cellulose with graphene oxide
M. El Achaby, N. El Miri, A. Snik, M. Zahouily, K. Abdelouahdi, A. Fihri, A. Barakat and A. Solhy, *J. Appl. Polym. Sci.* 2015, DOI: 10.1002/app.42356

Production and characterization of microfibrillated cellulose-reinforced thermoplastic starch composites
L. Lendvai, J. Karger-Kocsis, Á. Kmetty and S. X. Drakopoulos, *J. Appl. Polym. Sci.* 2015, DOI: 10.1002/app.42397

Development of bioplastics based on agricultural side-stream products: Film extrusion of *Crambe abyssinica*/wheat gluten blends for packaging purposes
H. Rasel, T. Johansson, M. Gällstedt, W. Newson, E. Johansson and M. Hedenqvist, *J. Appl. Polym. Sci.* 2015, DOI: 10.1002/app.42442

Influence of plasticizers on the mechanical and barrier properties of cast biopolymer films
V. Jost and C. Stramm, *J. Appl. Polym. Sci.* 2015, DOI: 10.1002/app.42513

The effect of oxidized ferulic acid on physicochemical properties of bitter vetch (*Vicia ervilia*) protein-based films
A. Arabestani, M. Kadivar, M. Shahedi, S. A. H. Goli and R. Porta, *J. Appl. Polym. Sci.* 2015, DOI: 10.1002/app.42894

Effect of hydrochloric acid on the properties of biodegradable packaging materials of carboxymethylcellulose/poly(vinyl alcohol) blends
M. D. H. Rashid, M. D. S. Rahaman, S. E. Kabir and M. A. Khan, *J. Appl. Polym. Sci.* 2015, DOI: 10.1002/app.42870

Journal of Applied Polymer Science

Combining polyhydroxyalkanoates with nanokeratin to develop novel biopackaging structures

Maria Jose Fabra, Pablo Pardo, Marta Martínez-Sanz, Amparo Lopez-Rubio, Jose M. Lagarón
Novel Materials and Nanotechnology Group, IATA-CSIC, Avda. Agustin Escardino 7, 46980 Paterna Valencia, Spain
Correspondence to: J. M. Lagaron (E-mail: lagaron@iata.csic.es)

ABSTRACT: This work reports on the combination of polyhydroxyalkanoate (PHA)-based materials and nanokeratin extracted from poultry feathers (a food by-product) using different approaches. In the first approach, high-barrier nanobiocomposites based on the combination of PHAs with a nanokeratin additive were successfully developed via both (i) direct melt compounding and (ii) preincorporated into an electrospun masterbatch of PHA which was subsequently melt compounded with PHA pellets. Enhanced barrier properties for the nanobiocomposites were obtained which were seen to depend on the PHA grade used. In the second approach, nanokeratin films were obtained via solution casting which were successfully hydrophobized by coating them with electrospun PHA fibers. The multilayered approach showed good adhesion and also lead to enhanced barrier performance. © 2015 Wiley Periodicals, Inc. J. Appl. Polym. Sci. **2016**, *133*, 42695.

KEYWORDS: biodegradable; biopolymers and renewable polymers; composites

Received 17 March 2015; accepted 9 July 2015
DOI: 10.1002/app.42695

INTRODUCTION

The interest in biodegradable disposable plastic items has steadily grown over the last decade. In this sense, there is a strong research interest, pushed by authorities at the national and international levels, and a parallel industrial growing demand in the development and use of biodegradable and renewable materials. Among the wide variety of biopolymers which have been developed and studied during the past years, biopolyesters such as polylactides (PLA)[1–3] and polyhydroxyalkanoates (PHA)[4] have attracted a special interest since they are synthesized from renewable resources and they can be processed using conventional melt compounding equipment.

PHAs are thermoplastic polyesters produced by a variety of bacteria as storage materials in response to particular stresses. Within this range of materials, the homopolymer poly(3-hydroxybutyrate) (PHB) has been more extensively studied since it presents mechanical properties similar to those of conventional petroleum-based polymers. Although PHB behaves similarly to conventional thermoplastics, it has relatively high glass transition and melting temperatures, leading to excessive brittleness. As an alternative, copolymers of PHB with hydroxyvalerate (known as PHBV) have been biotechnologically developed to improve the properties of this biopolyester, counteracting certain PHB drawbacks such as brittleness and poor processability.[5] However, they still present insufficient barrier to substitute other synthetic polymers commonly used for food packaging applications, such as poly(ethylene terephthalate) (PET).

In order to reduce energy consumption during the production of bioplastics and potential competition with agricultural resources for foods and also to provide additional raw material sources, the exploitation of food by-products is also a current trend. These by-products have rarely been used as a source of high added-value components such as food ingredients, but they present great potential value for their use in the production of biobased polymers. Therefore, biopolymers would have an added value when making use of by-products from the food industry which would permit the development of a new generation of packaging materials for food applications, with a revalorization of the biological constituents of the by-products. This is the case of whey protein, keratin, or cellulose obtained from milk, poultry feathers, or vegetal resources, respectively. For instance, the continuous and suitable growth of the poultry industry including increased poultry consumption is leading to an oversupply of by-products. These by-products are considered waste materials for the poultry industry and egg producers.

Natural derived proteins from gelatine, soybean, wheat, fish, corn, milk, wool, and poultry feathers have been processed into films using a variety of techniques.[6] Among them, keratin is a unique protein because it contains a large amount of the amino acid cysteine compared with other proteins. Cysteine is a sulfur-containing amino acid which can form intra- or intermolecular

sulfur–sulfur (S–S) bonds with other cysteine molecules. The intermolecular cysteine bonds together with other protein structural features, such as crystallinity and hydrogen bonding, give keratin high strength and stiffness.[6]

To the best of our knowledge, very few studies are reported on the use of keratin-based films or on the combination of keratin with biopolymers.[7,8] However, it is anticipated that keratin fillers and films may promote enhanced gas barrier properties for intermediate and low barrier matrices. For instance, Pardo *et al.*[9] showed that 1 wt % of microkeratin addition improved barrier properties of PHAs nanocomposites. However, high percentages (25–50 wt %) of microkeratin in PHA matrices could be only used in specific applications where the exchange of gases and/or water vapor is needed.

From an application point of view, it is of great relevance to diminish the water sensitivity of keratin, and to enhance the gas barrier properties and overall functionalities of thermoplastic biopolyesters like PHAs to make them more adequate for food packaging applications. To overcome these issues, two main approaches have been put forward in this work. The first one consists of the development of nanocomposite materials through the addition of nanofillers such as nanokeratin. In that case, nanofillers must provide a good matrix–filler adhesion and high nanofiller dispersion within the PHA matrix. As an alternative, the properties of PHAs can be modified by developing nanostructured multilayer systems.[9] One of the key issues to develop multilayer structures is to obtain sufficient adhesion between layers by using bioadhesives. In that case, the outer layers consist on good water vapor barrier biopolymers with good mechanical properties such as biopolyesters and the inner layer consists of biobased materials with good oxygen barrier properties such as proteins and polysaccharides.

Extensive research works have been performed in the study of biodegradable nanocomposites for food packaging applications. However, the so-called multilayer packaging systems which are widely used today for synthetic polymers are barely developed for biodegradable and renewable materials since it is difficult to assemble thermodynamically immiscible polymers or biopolymers without the addition of synthetic adhesives. Recently, Fabra *et al.*[10] have reported innovative strategies based on the electrohydrodynamic process to improve the barrier and functional performance of bio-based polymers by means of multilayering design, providing improved adhesion between the different packaging layers. The electrohydrodynamic process, also known as electrospinning, is a technique which makes use of high-voltage electric fields to produce electrically charged jets from viscoelastic polymer solutions which on drying, by the evaporation of the solvent, produce ultrathin polymeric structures.

In a recent work, Pardo *et al.*[9] developed novel biodegradable and renewable composite materials based on the combination of PHAs with a microkeratin fibers prepared from milled poultry feathers. In this study, novel composite materials have been carried out to improve barrier properties of PHA materials with a food by-product. On the one hand, high-barrier nanobiocomposites based on the combination of PHAs with a nanokeratin additive were developed via both (i) direct melt compounding and (ii) preincorporation into an electrospun masterbatch of PHA which was subsequently melt compounded with PHA pellets. This preincorporation method was previously developed and successfully applied to enhance the properties of the PHBV matrices with nanocellulose.[11] On the other hand, nanokeratin films were obtained via solution casting which were hydrophobized by coating them with electrospun PHA fibers to retain the good gas barrier properties of keratin at high humidity, i.e., in real packaging application. This methodology has been previously developed and applied to hydrophobize wheat gluten films.[10]

MATERIALS AND METHODS

Materials

The bacterial PHA was a melt-processable semicrystalline grade purchased from Goodfellow Cambridge Limited, U.K., in pellet form (density 1.25 g/cm^3). This grade (from now on referred to as PHBV12) consisted of a poly(3-hydroxybutyrate-co-3-hydroxyvalerate) polymer containing 12 mol % hydroxyvalerate (HV) plasticized with 10 wt % of citric ester. PHBV3 with 3 mol % HV was supplied in pellet form by Tianan Biopolymer, Ningbo (China). Both PHAs were used as polymer matrices of nanocomposites and as nanostructured coatings in the multilayer systems.

Poultry feathers were kindly supplied by Mayava, S.L. (Valencia, Spain). Feathers were firstly sanitized with a bath in ethanol (96%), 1 : 2 feathers-to-ethanol ratio in mass, followed with a second bath in ethanol (70%) using the same ratio. Afterward, feathers were dried overnight at 50°C.

2,2,2-Trifuoroethanol (TFE) with 99% purity were purchased from Sigma-Aldrich (Spain) and it was used as a solvent for the PHBV3 and PHBV12. All products were used as received without further purification.

Keratin Nanoadditive Preparation

First, keratin was extracted from poultry feathers following the methodology previously described by Schrooyen *et al.*, 2000.[12] Briefly, 35 g of feathers were added to 500 mL of an aqueous solution containing 8 M urea, 3 mM EDTA, 125 mM 2-mercaptoethanol, and 200 mM Tris-buffer, pH 9.0 and the mixture was kept at 70°C under vigorous stirring. After 2 h, the suspension was vacuum filtered to isolate the liquid. Then, the liquid was dialyzed against purified water using a 10 kDa membrane. Three dialysis cycles of 24 h were completed to eliminate the species in solution, obtaining a stable 3% (w/v) keratin suspension. Finally, droplets of the suspension were flash-frozen by using liquid nitrogen and, subsequently freeze-dried at a pressure of 10^{-4} atm in a Telstar Cryodos freeze-drier (Terrasa, Spain) to produce a loose very fine powder, referred to as nanokeratin. Particle size distribution was determined from nanokeratin aqueous dispersions by dynamic light scattering using a Malvern Zetasizer Nano analyzer.

Electrospinning of Hybrid PHA–Nanokeratin Fibers

Electrospun hybrid fibers were generated from PHBV3–nanokeratin suspensions in 2,2,2-trifluorethanol. The electrospinning suspensions contained a total solids concentration of 6 wt %

and the nanokeratin concentration was 15%, 30%, and 50% (w/w) with respect to the PHBV3 mass. The dry nanokeratin powder was dispersed in the solvent by applying intense homogenization (Ultraturrax) for 5 min and it was then stirred with the PHBV3 at 60°C until complete dissolution of the polymer.

The electrospinning apparatus used was the high-throughput Fluidnatek® LE500 tool manufactured by Bioinicia S.L., Valencia (Spain) operated in the laboratory mode. A high-voltage 0–60 kV power supply operating at 10–12 kV was used and the polymer solution was fed into the emitter at a rate of 0.70 mL/h. The distance between the emitter and the collector was 10 cm and the experiments were carried out at ambient temperature.

Preparation of PHA–Nanokeratin Composites by Melt Compounding

Nanocomposite PHAs films were prepared by melt compounding using two different approaches: (i) the traditional method of melt mixing of the polymeric matrix with the dry nanofiller, and (ii) by blending the PHA pellets with PHA–nanokeratin masterbatches produced by electrospinning.

For the conventional approach, the nanokeratin powder was directly melt mixed with the PHBV3 and PHBV12 matrices in concentrations ranging from 0 to 5 wt %. Alternatively, the required amount of hybrid electrospun PHBV3 fibers produced from suspensions containing 30 wt % nanokeratin were melt mixed with PHBV3 pellets to produce nanocomposites with final nanofiller concentrations of 1 and 3 wt %.

The melt-mixing step was carried out in a Brabender Plastograph mixer (16 cm^3) for 4 min at 175 and 160°C for PHBV3 and PHBV12, respectively. The mixing temperature was carefully selected to avoid excessive thermal exposure of the nanokeratin while being high enough to melt the PHAs. After mixing, the batches were left at room temperature to cool down.

Finally, *ca* 0.3 g of the blends were sandwiched between glass fiber reinforced PTFE foils using a 25 cm^2 template of the same material. A pressure of 35 MPa was applied for 4 min at 165°C using a Carver hot-plate hydraulic press.

Preparation of Nanokeratin-Based Multilayer Systems

Preparation of Nanokeratin Films. First, nanokeratin films were produced from the aqueous suspensions obtained after the dialysis cycles described in the section titled "Keratin Nanoadditive Preparation". Approximately 75 mL of these suspensions were cast onto plastic Petri dishes and dried at 30°C during 2–3 days. These films were used as inner layer of the multilayer systems.

Preparation of Multilayer Systems. In order to protect the highly hydrophilic nanokeratin layer, this film was coated with PHBV3 and PHBV12 mats produced by means of the electrospinning technique. PHBV3 and PHBV12 solutions in 2,2,2-trifluorethanol having a total solids content of 6 wt % were used to generate the electrospun fibers using the same setup as described in the section titled "Electrospinning of Hybrid PHA–Nanokeratin Fibers", with a voltage of 10–12 kV and a feeding rate of 0.66 mL/h. In this case, the collector was a nanokeratin film. Both sides of the nanokeratin film were coated. The distance between the emitter and the film to be coated was 8 cm and the experiments were carried out at ambient temperature.

Electrospun coatings presented an opaque and whitish appearance. With the aim of obtaining transparent and continuous pellicles, an additional heating step was applied. Coated films were placed in between hot plates at 160°C during 2 min (without pressing) to melt and homogenize the electrospun PHBV3 or PHBV12 phase.

Transmission Electron Microscopy (TEM)

Ultrathin sections of microtomed thin composite sheets were observed by TEM. The samples were stained with a 2 wt % solution of uranyl acetate. TEM was performed using a JEOL 1010 equipped with a digital Bioscan (Gatan) image acquisition system at 80 kV.

Scanning Electron Microscopy (SEM)

SEM was conducted on a Hitachi microscope (Hitachi S-4800) at an accelerating voltage of 5 KV and a working distance of 12–16 mm. A droplet of the nanokeratin suspension was dried on a sample holder to characterize the nanoadditive morphology. Additionally, electrospun fibers and films cryofractured after immersion in liquid nitrogen were sputtered with a gold–palladium mixture under vacuum before their morphology was examined using SEM.

FT-IR Analysis

Transmission FT-IR experiments were recorded in a controlled chamber at 21°C and 40% RH (relative humidity) using a Bruker (Rheinstetten, Germany) FT-IR Tensor 37 equipment. The spectra were taken at 1 cm^{-1} resolution averaging a minimum of 10 scans. Analysis of the spectra was performed using Grams/AI 7.02 (Galactic Industries, Salem, NH, USA) software.

Samples of *ca* 0.5 mg from the nanokeratin additive and the hybrid PHBV3–nanokeratin electrospun fibers were ground and dispersed in 200 mg of spectroscopic grade KBr. A pellet was then formed by compressing the sample at *ca* 150 MPa. To estimate the amount of nanokeratin effectively incorporated into the hybrid electrospun fibers, a calibration curve was obtained by recording the IR spectra of pellets containing 0.5 mg of PHBV3–nanokeratin samples with known amounts of PHBV3 electrospun fibers and nanokeratin. The so-prepared standard samples contained concentrations of 20, 40, and 60 wt % nanokeratin.

The intensity ratio of the bands located at 1650 cm^{-1} (characteristic from the amide I group in the nanokeratin) and 1730 cm^{-1} (characteristic from the carboxyl group in the PHBV matrix) was calculated for the standard samples and the results were plotted against the known concentration of nanokeratin, obtaining the calibration curve shown below. This calibration curve was subsequently used to estimate the amount of nanokeratin incorporated into the hybrid electrospun fibers by estimating the corresponding I_{1650}/I_{1730} values from the FT-IR spectra ($R^2 = 0.9972$).

Differential Scanning Calorimetry (DSC)

Differential scanning calorimetry of PHAs and its composites was performed on a Perkin-Elmer DSC 7 thermal analysis system on typically 7 mg of material at a scanning speed of 10°C/min. Two heating scans were carried out from −40 to 170°C separated with a cooling scan at the same rate. The baseline of the thermograms was corrected with similar runs of an empty pan and the DSC equipment was calibrated with an indium standard.

Crystallinity was estimated using the ratio between the heat of fusion of the studied material and the heat of fusion of a perfect crystal of same material, i.e.,

$$\%Xc = \frac{\Delta H_f}{\Delta H_f^0} \cdot 100 \quad (1)$$

Where ΔH_f is the enthalpy of fusion of the studied specimen and ΔH_f^0 is the enthalpy of fusion of a totally crystalline material ($\Delta H_f^0 = 146$ J/g for PHBV[13]).

Water Vapor Permeability (WVP)

WVP was measured in film discs ($\phi = 3.5$ cm) according to the ASTM 2011[14] gravimetric method, using Payne permeability cups (Elcometer SPRL, Hermelle/s Argenteau, Belgium). For nanocomposites films, distilled water was placed inside the cup to expose the film to 100% RH on one side. However, for the pure nanokeratin-based films and multilayer systems, oversaturated solutions of NaCl was placed inside the cup to expose the film to 75% instead of 100% RH since the nanokeratin film was partially dissolved when 100% was used. In both cases, each cup was placed in cabinets at 25°C and 0% of relative humidity to establish a 0–100% and 0–75% RH gradient for nanocomposites and multilayer structures, respectively. The RH of the cabinet was kept constant using silica gel. The cups were weighed periodically (±0.0001 g). Cups with aluminum films were used as control samples to estimate solvent loss through the sealing. Water vapor permeation rate was calculated from the steady-state permeation slopes obtained from the regression analysis of mass loss data *vs* time, and mass loss was calculated as the total cell loss minus the loss through the sealing. Permeability was obtained by multiplying the permeance by the average film thickness.

Oxygen Permeability

The oxygen permeation rate of samples was determined at 80% RH and 25°C using an Oxtran 100 equipment (Modern Control Inc., Minneapolis, MN, US). Relative humidity of 80% was generated by a built-in gas bubbler and was checked with a hygrometer placed at the exit of the detector. Samples were purged with nitrogen for a minimum of 20 h in the previously relative humidity equilibrated samples, prior to exposure to an oxygen flow of 10 mL min^{-1}. The exposure area during the test was 5 cm^2 for each sample. In order to obtain the oxygen permeability, film thickness was considered in each case.

Tensile Testing

Tensile tests were carried out at ambient conditions typically at 24°C and 50% RH on an Instron 4400 Universal Tester. Preconditioned dumb-bell-shaped specimens with initial gauge length and width of 25 and 5 mm were die-stamped from the films in the machine direction according to the ASTM D638.[15] A fixed cross-head rate of 10 mm/min was utilized in all cases and results were taken as the average of, at least, four tests.

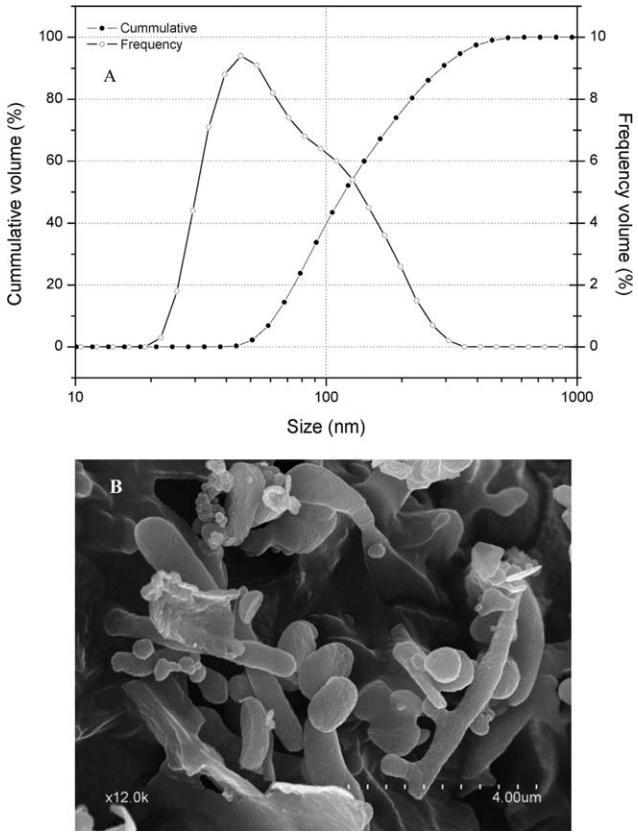

Figure 1. (A) Particle size distribution and (B) SEM micrograph of the nanokeratin additive.

Contact Angle Measurements

Measurements of contact angle were performed in a Video-Based Contact Angle Meter model OCA 20 (Data Physics Instruments GmbH, Filderstadt, Germany) at 25°C and ambient relative humidity (ca. 53% RH). Contact angle measurements were obtained by analyzing the shape of a distilled water drop after it had been placed over the film for 5 s. Image analyses were carried out by SCA20 software. Results were taken as the average of, at least, 10 tests.

Statistical Analysis

One-way analysis of the variance (ANOVA) was performed using Statgraphics 5.1 software package. Comparisons between samples were evaluated using the Tukey test.

RESULTS

Development of Nanokeratin/PHBV Composites

Nanokeratin Characterization and Production of Hybrid PHBV Electrospun Fibers. During the first part of this work, keratin nanoadditives were extracted from chicken feathers to be used as a filler in PHAs-based nanocomposites. The study of the morphology and particle size distribution of the nanoadditives is of interest since they are known to affect the nanofiller reinforcing effect when incorporated into a polymeric matrix.[16] Figure 1(A) shows the cumulative curve of the particle size

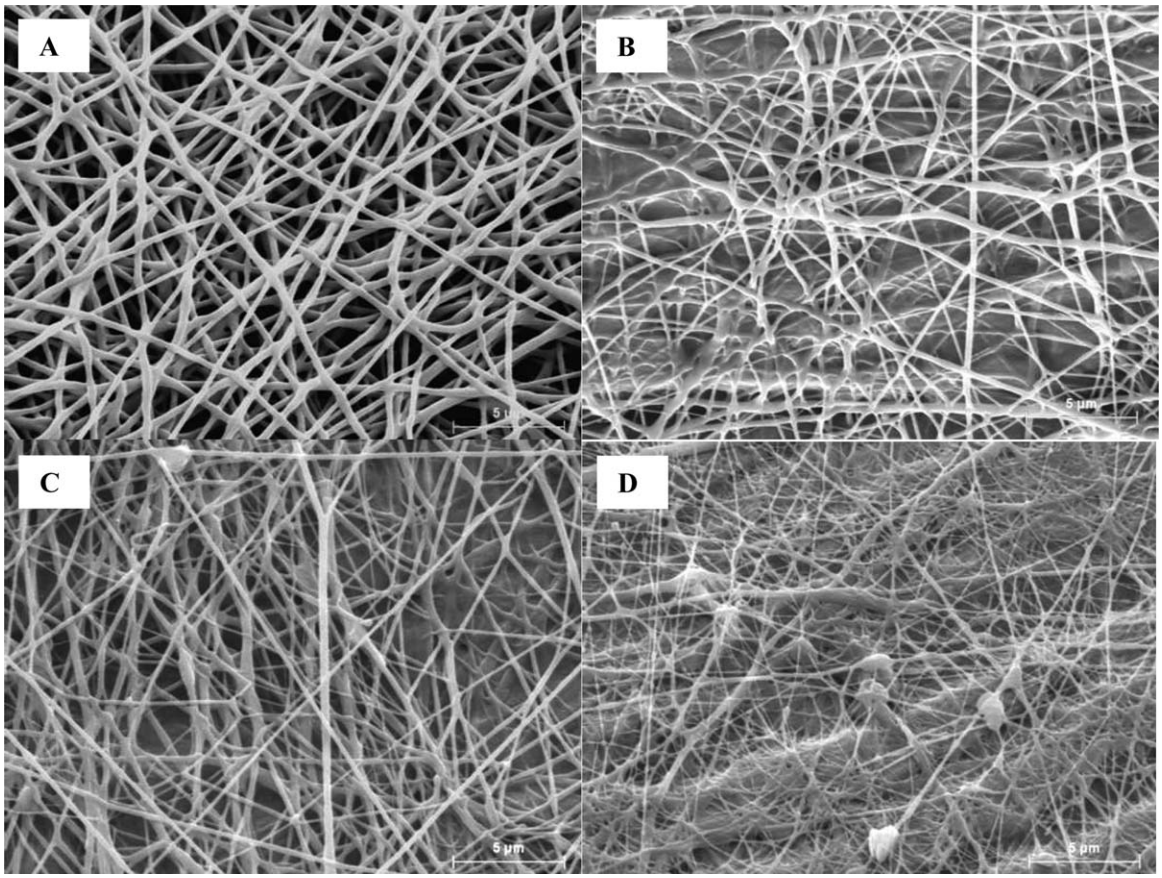

Figure 2. SEM micrographs of electrospun fibers produced from 6 wt % solutions in TFE: (A) PHBV3 (published in Martínez-Sanz *et al.*[11]); (B) PHBV3 + 15% nanokeratin; (C) PHBV3 + 30% nanokeratin; and (D) PHBV3 + 50% nanokeratin.

distribution of the keratin nanoadditive analyzed by means of dynamic light scattering. Although the nanokeratin showed a wide size distribution, 50% of the volume of the sample and the maximum frequency in number was <100 nm, hence the term nanokeratin used for the material. SEM observation of the aqueous nanokeratin suspensions after drying by casting [cf. Figure 1(B)] shows that nanokeratin particles presented different morphologies such as fibrillar and spherical nanoparticles.

The main objective of this work was to evaluate the potential of the extracted nanokeratin as a barrier material, incorporating it as an additive to produce nanocomposite materials by melt compounding and using it to produce multilayer systems based on the combination of nanokeratin films with PHA coatings.

With regard to the production of PHA–nanokeratin composites, two different strategies were followed to incorporate the nanoadditive into the PHA matrices by the melt compounding process. The traditional method of direct blending the additive with the matrix was followed to produce PHBV3 and PHBV12 nanocomposite films. Alternatively, the nanokeratin was preincorporated into PHBV3 by means of electrospinning to generate masterbatches which were subsequently melt mixed with PHBV3 pellets, i.e., the so-called electrospinning enabling melt compounding route. This approach has been previously shown to significantly improve the dispersion of nanoadditives such as cellulose nanowhiskers, hence leading to enhanced barrier properties of the resulting nanocomposites.[17]

First of all, the production of electrospun hybrid PHBV3–nanokeratin fibers was previously optimized and used as a benchmark[11] to maximize the incorporation of nanoadditive into the fibers. Using the same conditions, electrospun fibers were prepared from solutions with increasing nanokeratin concentrations (15, 30, and 50% (w/w) with respect to the PHBV3 mass). The morphology of the so-obtained fibers is shown in Figure 2 and compared to the pure PHBV3 fibers.[11] As observed, more heterogeneous structures were attained as the concentration of the nanokeratin was increased.

It has been previously demonstrated that when electrospun fibers are produced from heterogeneous polymer–nanofiller suspensions, the degree of nanoadditive incorporation may be lower than expected. To estimate the degree of incorporation from the three different solutions used, a calibration curve was built by preparing KBr pellets with known concentrations of keratin and PHBV3 and measuring the ratio of the band located at *ca* 1670 cm^{-1} (characteristic from the amide I group in the nanokeratin) and the band appearing at *ca* 1730 cm^{-1} (characteristic from the carboxyl group in the PHBV matrix).[9] The spectra of the three different hybrid fibers produced were then recorded [cf. Figure 3] and the nanokeratin incorporation

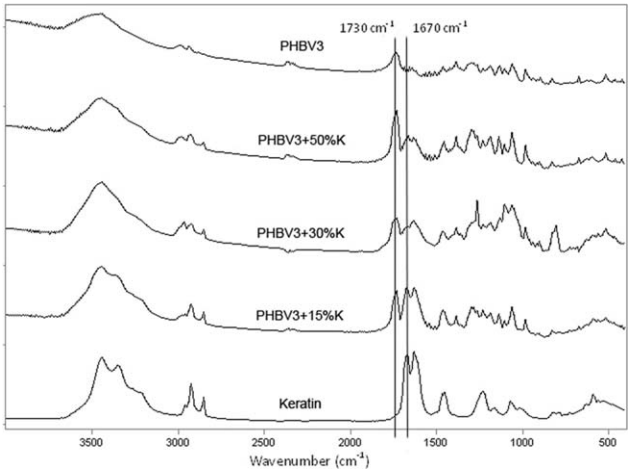

Figure 3. FT-IR spectra of the nanokeratin additive and of pure and hybrid PHBV3 electrospun fibers.

degree was estimated as *ca* 15, 26, and 32%. Due to the inefficient incorporation of the nanoadditive when increasing the nanokeratin concentration to 50%, suspensions with 30% nanokeratin were considered as the optimum to synthesize the hybrid fibers.

Chacterization of PHBV–Nanokeratin Composites by Melt Compounding. After the nanokeratin production and preincorporation, the required amount of hybrid electrospun fibers were incorporated into PHBV3 by melt compounding to produce nanocomposites with optimal nanofiller dispersion. This approach was compared to the direct melt mixing approach and the morphology of the so-obtained nanocomposites was investigated by SEM of the cryofractured cross-sections, as displayed in Figure 4. Nanokeratin aggregates were detected in the nanocomposites with concentrations higher than 3 wt %. For lower filler loadings, best dispersion and distribution were achieved which degree depended on the incorporation strategy

Table I gathers the thermal properties of PHBV3 and PHBV12 nanocomposite films as determined from DSC analyses. The melting temperatures (T_{m1} and T_{m2}) and the corresponding melting enthalpies values (ΔH_{m1} and ΔH_{m2}) normalized to the PHBV3 or PHBV12 content of the nanocomposites films were obtained from DSC first heating run. As deduced from the results, both grades presented two melting peaks, just as reported in previous works.[9,18] This behavior has been explained by the fact that more defective and smaller crystals melted and subsequently recrystallized, forming more perfect crystals, which melted at higher temperature.[18,19]

In general, the thermal properties of PHBV3 and PHBV12 were not strongly affected by the nanokeratin addition. As observed, the melting point was not affected or just showed slight variations along the whole range of additions for both heating runs. Therefore, this discards severe filler-induced polymer degradation phenomena, which has been reported for PHBV composites containing nanoclays.[20] It may be noted that nanocomposite films prepared by means of the preincorporation method did not show a second melting point which can be ascribed to a better dispersion and/or distribution of the filler that may in turn affect the crystalline morphology of the polymer, improving the better barrier performance of these nanocomposites films as compared to their counterparts prepared by direct melt-compounding process (without preincorporation). In fact, although no significant differences were found on the crystallization temperature (T_c), it can be observed a tendency to decrease T_c values in nanocomposites prepared with the preincorporation method.

It should be noted that the melting enthalpy was not modified by the nanokeratin addition, which indicates that nanofillers did not affect the crystallization of the PHA matrices. Similar effects were observed for PHBV12 nanocomposites containing plant-derived cellulose nanowhiskers which were obtained via solution casting.[21] The results are in agreement with Pardo-Ibañez *et al.*[9] who reported that for up to 3 wt % of microkeratin addition, crystallinity was not modified. However, they found that greater additive content led to a drop in the crystallinity index, indicating that the presence of greater microkeratin fiber contents significantly hindered the crystallization process.

Tensile properties of PHAs and their nanocomposites are summarized in Table II. The typical stress–strain curves of PHBV12 nanocomposites are displayed in Figure 5. Similar curves were observed for PHBV3. From these results, it can be deduced that when increasing the valerate content of PHAs, the elastic modulus, and tensile strength decreased, whereas the elongation at break increased. This behavior has been previously reported in several studies[22,23] and is in accordance with DSC analysis, which showed lower crystallinity degree for PHBV12 nanocomposites. This could be indicative of the increased segmental mobility in the amorphous phase and thus, of reduced brittleness for the higher valerate PHA. As observed in Table II, no clear trend was observed for PHBV3 and PHBV12 nanocomposites with the addition of nanokeratin, although slight differences were observed in the elongation at break values due to the incorporation strategy. The traditional method of direct blending the additive with the matrix gave rise to more brittle nanocomposites, whereas the preincorporation method did not significantly modify the stretchability of the developed PHBV3–nanocomposites.

To the best of our knowledge, the effect of nanokeratin on the transport properties of PHAs has not been previously investigated. Table III summarizes the water and oxygen permeability values of the pristine melt-mixed PHBV3 and PHBV12 and their nanocomposites with 0.5, 1, 3, and 5 wt % of nanokeratin. The permeability values of both PHA materials are in agreement with those reported in the literature for melt-compounded films.[24] The first observation to highlight is that the effect of nanokeratin addition on the barrier properties was somewhat different depending on the PHA grade. For PHBV3 nanocomposites, 0.5 wt % was the optimum loading in terms of oxygen and water barrier reinforcing properties but the permeability drop (mainly water vapor) decreased with increasing nanokeratin content. At a given nanokeratin loading, the

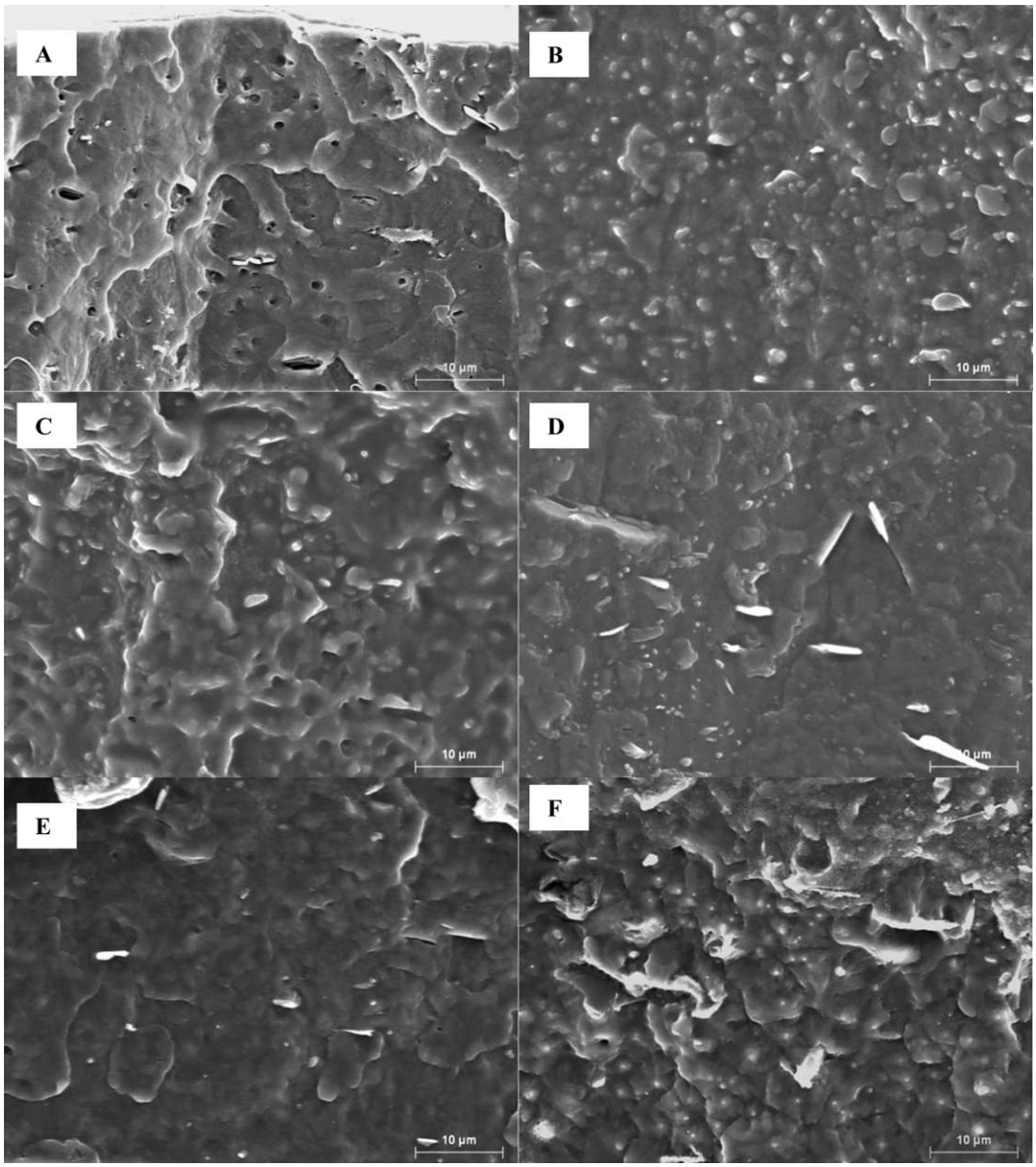

Figure 4. SEM micrographs of the cryofractured section obtained from PHBV nanocomposite films: (A) Pure PHBV3; (B) PHBV3 + 1% nanokeratin; (C) PHBV3 + 3% nanokeratin; (D) PHBV3 + 5% nanokeratin; (E) PHBV3 + 1% nanokeratin (through electrospun fibers); and (F) PHBV3 + 3% nanokeratin (through electrospun fibers). Scale markers correspond to 10 μm.

preincorporation method improved water vapor and oxygen permeability of the developed nanocomposites.

For the PHBV12 composite materials with nanokeratin loadings higher than 0.5 wt %, a reduced water and oxygen permeability as compared to the neat PHBV12 was obtained. For PHBV12, an optimum additive percentage was observed at 3 wt % nanokeratin addition, resulting in a water vapor and oxygen permeability reductions of ~63% and ~73%, respectively. In principle, nanokeratin fillers are hydrophilic and swell in the presence of water, dropping barrier performance; however when confined in a more hydrophobic matrix (PHAs), they may actually undergo a resistant to swelling and hence plasticization. To further investigate the dispersion of the nanofiller within the matrix, the PHBV12 nanocomposite film with 3 wt % nanokeratin loading was examined by TEM and a representative image is shown in Figure 6. The TEM image confirmed a relatively good nanofiller dispersion and distribution within the PHBV12 matrix as well as a good adhesion between the nanofiller and the biopolyester. Although no statistically significant differences were found between 3 and 5 wt % because of the high standard deviations, a trend of increasing water and oxygen permeability values were observed when incorporating nanokeratin in higher loadings.

There is very scarce literature reporting on the water and oxygen barrier properties of PHA-based nanocomposites reinforced with nanoadditives. Pardo-Ibañez *et al.*[9] observed water permeability reduction of up to 58% for PHBV12 matrices reinforced with 1 wt % microkeratin via solution casting. Martínez-Sanz

Table I. DSC Maximum of Melting (T_{m1} and T_{m2}) and the Corresponding Melting Enthalpies (ΔH_{m1} and ΔH_{m2}), Degree of Crystallinity (X_c), and Crystallization Temperature (T_c) of Melt-Mixed PHBV12 and Its Nanocomposites with 0.5, 1, 3, and 5 wt % of Nanokeratin. Mean Value (Standard Deviation)

	PHBV3					PHBV12				
Nanokeratin (%)	T_{m1} (°C)	T_{m2} (°C)	ΔH (J/g PHBV3)	X_c (%)	T_c (°C)	T_{m1} (°C)	T_{m2} (°C)	ΔH (J/g PHBV12)	X_c (%)	T_c (°C)
0	168.9 (0.5)[a]	183.6 (0.1)[a]	73.2 (5.0)[a]	50.1 (3.4)[a]	112.8 (0.5)[a]	139.9 (0.8)[a]	153.6 (0.8)[a]	38.9 (0.9)[a]	26.7 (0.6)[a]	102.7 (0.4)[a]
0.5	168.4 (1.6)[a]	183.5 (0.1)[a]	82.8 (3.1)[ab]	56.4 (2.1)[a]	112.6 (0.6)[a]	135.5 (1.7)[a]	152.2 (0.7)[a]	34.1 (2.0)[ab]	23.2 (1.4)[a]	101.2 (0.4)[a]
1	170.4 (1.4)[a]	183.9 (0.2)[a]	80.7 (8.5)[a]	54.7 (5.8)[a]	114.1 (0.5)[a]	138.1 (1.1)[a]	152.9 (0.4)[a]	37.6 (0.2)[a]	25.5 (0.1)[a]	102.5 (0.5)[a]
3	168.6 (1.8)[a]	183.9 (0.2)[a]	81.2 (5.8)[a]	54.0 (3.8)[a]	112.7 (0.6)[a]	141.3 (1.1)[a]	154.2 (1.2)[a]	33.8 (1.4)[a]	22.4 (0.9)[a]	102.6 (0.7)[a]
5	170.0 (0.6)[a]	183.9 (0.7)[a]	75.1 (0.9)[a]	49.0 (0.6)[a]	114.6 (0.5)[a]	138.0 (0.2)[a]	152.7 (0.2)[a]	37.7 (0.1)[a]	24.6 (0.1)[a]	102.6 (0.4)[a]
1 ES	171.8 (3.2)[a]	-	79.2 (3.9)[a]	54.2 (2.7)[a]	113.5 (0.7)[a]	-	-	-	-	-
3 ES	167.8 (0.1)[a]	-	81.7 (1.4)[a]	56.0 (0.9)[a]	109.4 (0.6)[a]	-	-	-	-	-

[a,b] Different superscripts within the same column indicate significant differences among nanocomposites.
[a] ES refers to those obtained by using the preincorporation method (electrospinning) and the number before the ES indicates the content.

et al.[21] reported increased water permeability values when cellulose nanowhiskers were incorporated into PHBV12 matrix obtained by the casting method. However, a previous work in which PHBV12 films loaded with purified cellulose microfibers were produced by casting, reported optimum barrier properties for a loading of 1 wt % cellulose microfibers, showing a water permeability decrease of 71%.[25] Therefore, the effect of nanofillers highly depends on the nature of both the reinforcing agents and the polymer matrix. In other works, Sánchez-García and Lagaron[26] observed oxygen permeability reductions of up to 21% for PHA reinforced with 4% (w/w) layered silicates and Martínez-Sanz *et al.*[9,21] reported oxygen permeability reductions of 26–27 and 28–44% for the nanocomposites containing 1–2% of wheat straw cellulose nanowhiskers and brewers spent grain cellulose nanowhiskers, respectively.

Therefore, the results here obtained demonstrated that nanokeratin was more efficient in enhancing both oxygen and water vapor barrier properties of PHAs nanocomposite films than other nanofillers widely used to improve barrier properties of biopolyesters. For a given nanokeratin concentration, PHBV3 nanocomposites prepared by the preincorporation method were more deformable and had reduced water vapor and oxygen permeability as compared to the traditional method of directly blending the nanoadditive with the matrix.

Barrier Performance of PHA-Coated Keratin-Based Films

The purpose of the second part of this work was to develop nanokeratin films and to enhance the performance of this material at high relative humidity by coating them with hydrophobic layers via the electrohydrodynamic process previously described by Fabra *et al.*[10] Two different PHAs, with different valerate contents (3 and 12%), were used as coating layers.

Regarding the mechanical properties of the multilayer films, as observed in Table IV and Figure 7, PHBV3 strongly affected the mechanical performance of the neat nanokeratin film, whereas PHBV12 coatings did not significant modify the tensile properties of the nanokeratin inner layer. When the nanokeratin film was coated with the annealed PHBV3 electrospun nanostructured fibers, the multilayer systems presented higher elastic modulus and tensile strength but lower elongation at break. Therefore, the mechanical response of the multilayer systems was greatly influenced by the semicrystalline nature of the outer PHA materials. As previously observed in Tables I and II, PHBV3 is more crystalline, mechanically stiffer, stronger, and less ductile than PHBV12.

As shown in Figure 8, the nanokeratin film presented a dense and compacted structure which was held by the strong hydrogen network established between the hydroxyl groups present on the keratin chains. WVP of the nanokeratin film was 4.53 ± 1.15 e^{-14} (kg m s^{-1} m^{-2} Pa^{-1}), which was similar to that previously reported for hydrophilic films such as sodium caseinate[27] and starch.[28] However, it was not possible to measure; it provided an average in the test, the oxygen permeability of the pure nanokeratin films since the material partially disintegrated when subjected to the high relative humidity conditions (80% RH) used for the standard oxygen permeability measurements. Protein-based films have been proved to have

Table II. Young's Modulus, Tensile Strength, and Elongation at Break for PHBV and Its Nanocomposites Incorporating Nanokeratine

	PHBV3			PHBV12		
Nanokeratin (%)	*E* (GPa)	Tensile strength (MPa)	ε_b (%)	*E* (GPa)	Tensile strength (MPa)	ε_b (%)
0	2.32 (0.12)^{a}	30.67 (1.24)^{a}	1.90 (0.10)^{a}	0.78 (0.05)^{a}	21.07 (1.03)^{a}	5.90 (0.30)^{a}
0.5	1.75 (0.16)^{a}	22.74 (7.04)^{ab}	0.80 (0.20)^{b}	0.84 (0.01)^{a}	17.68 (0.27)^{ab}	4.01 (0.01)^{b}
1	1.55 (0.07)^{a}	18.19 (2.48)^{b}	0.70 (0.40)^{b}	0.82 (0.04)^{a}	20.39 (1.31)^{a}	5.32 (0.60)^{a}
3	1.84 (0.25)^{a}	21.53 (8.03)^{ab}	0.93 (0.15)^{b}	0.94 (0.05)^{a}	17.64 (0.76)^{ab}	4.01 (0.40)^{b}
5	1.71 (0.18)^{a}	21.03 (1.22)^{b}	1.10 (0.40)^{ab}	0.77 (0.03)^{a}	15.52 (0.80)^{b}	3.25 (0.15)^{b}
1 ES	1.64 (0.05)^{a}	30.15 (1.85)^{a}	2.00 (0.15)^{a}	-	-	-
3 ES	1.66 (0.13)^{a}	26.31 (3.71)^{ab}	1.82 (0.20)^{a}	-	-	-

^{a,b} Different superscripts within the same column indicate significant differences among nanocomposites.
ES refers to those obtained by using the preincorporation method (electrospinning).

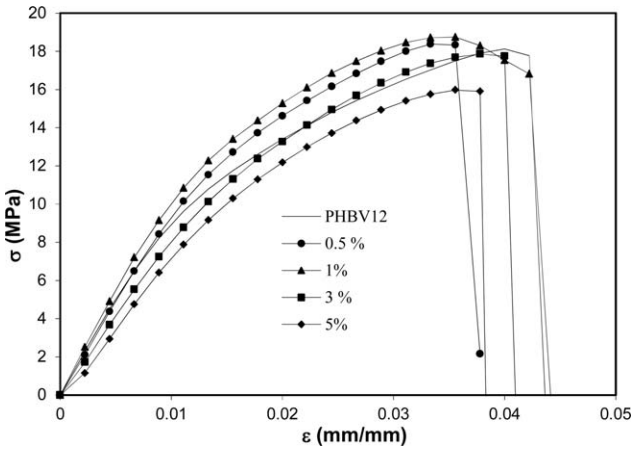

Figure 5. Typical stress–strain curves of the PHBV12 nanocomposites films.

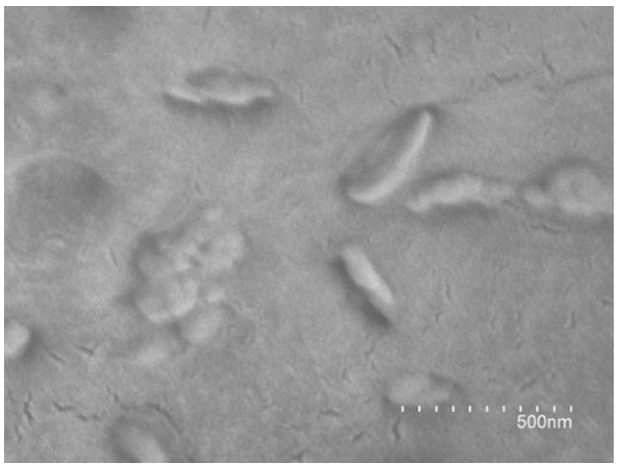

Figure 6. TEM image of the PHBV12 nanocomposite film containing 3% wt nanokeratin.

excellent oxygen barrier properties in dry conditions; however, when exposing these materials to high relative humidity conditions, the oxygen permeability increases dramatically. This behavior is typical of hydrophilic materials and it is ascribed to the plasticization effect caused by water vapor molecules sorbed within the amorphous nanokeratin domains. Figure 6 also shows a detail of the laminar-like structure of nanokeratin films coated with PHBV3 in which a very good adhesion between layers was observed. This structure must surely affect the barrier properties of the overall multilayer systems.

Table V gathers the barrier properties of pure nanokeratin and their nanostructured multilayer systems. The first clear

Table III. Oxygen and Water Vapor Permeability Values of Melt-Mixed PHBV12 and Its Nanocomposites with 0.5, 1, 3, and 5 wt % of Nanokeratin. Mean Value (Standard Deviation)

	WVP $_{(0\text{-}100\%\ RH)}$ (kg m s^{-1} m^{-2} Pa^{-1})		O_2P $_{(80\%\ RH)}$ (m^3 m m^{-2} s^{-1} Pa^{-1})	
Nanokeratin (%)	PHBV3	PHBV12	PHBV3	PHBV12
0	3.54 (0.40) e^{-15a}	1.14 (0.27) e^{-14a}	1.75 (0.25) e^{-19a}	3.04 (0.05) e^{-18a}
0.5	1.22 (0.10) e^{-15b}	1.05 (0.12) e^{-14a}	1.21 (0.27) e^{-19a}	1.92 (0.39) e^{-18a}
1	3.48 (0.55) e^{-15a}	0.62 (0.01) e^{-14b}	1.06 (0.21) e^{-19a}	2.03 (0.06) e^{-18b}
3	2.24 (0.21) e^{-15a}	0.42 (0.13) e^{-14c}	1.09 (0.63) e^{-19a}	0.83 (0.04) e^{-18c}
5	2.62 (0.20) e^{-15a}	0.64 (0.19) e^{-15c}	2.08 (0.25) e^{-19a}	1.36 (0.30) e^{-18c}
1 ES	2.30 (0.02) e^{-15c}	-	0.90 (0.05) e^{-19b}	-
3 ES	1.59 (0.05) e^{-15b}	-	1.00 (0.03) e^{-19a}	-

$^{a-c}$ Different superscripts within the same column indicate significant differences among nanocomposites.

Table IV. Young's Modulus, Tensile Strength, and Elongation at Break for the Pure Keratin Film and the Multilayer PHAs Coated Systems

	E (MPa)	Tensile strength (MPa)	ε_b (%)
Nanokeratin	38.73 (16.80)[a]	2.96 (0.17)[a]	70.50 (54.93)[a]
Nanokeratin–PHBV3	272.83 (77.78)[b]	8.53 (1.63)[b]	4.67 (0.32)[b]
Nanokeratin–PHBV12	23.56 (17.11)[a]	1.46 (0.30)[a]	130.15 (77.07)[a]

[a,b] Different superscripts within the same column indicate significant differences among nanocomposites.

observation is that when coating nanokeratin films with annealed PHBV3 and PHBV12 electrospun nanostructured fibers, water permeability dropped by *ca* 63% and 40%, respectively, thus providing greater water barrier properties. Interestingly, multilayer structured prepared with PHBV3 as a coating layer showed the best improvements in oxygen and water vapor permeability values mainly due to decreased water sorption (*cf.* Table V). As it is reported in the literature,[25] PHA films with lower valerate content had higher crystallinity degree than the high valerate content films and this is in agreement with previous studies which also corroborated that the lower crystallinity of higher valerate PHA polymers led to increased water permeability.[29] Multilayer structures prepared with PHBV12 seemed to be more affected by the presence of moisture, thus providing lower barrier than the PHBV3.

The wettability properties of the nanokeratin films and the coated multilayer systems were determined by direct measurement of contact angles of a water drop deposited on the upper surface of samples in order to investigate the effect of the PHBV3 and PHBV12 outer layers on the surface water affinity. The contact angle of the nanokeratin film was 35.2 ± 1.9° and, as expected, it was characteristic of hydrophilic materials. However, coating of nanokeratin films with annealed biopolyester electrospun nanostructured fibers resulted in more hydrophobic materials with contact angle values of 82.5 ± 1.6° and 80.1 ± 3.0° for PHBV3 and PHBV12, respectively.

CONCLUSIONS

This work demonstrated that it is possible to obtain nanokeratin from poultry feathers which can be used both as reinforcing agent in nanocomposite films and as a nanokeratin film layer protected by more hydrophobic nanostructured polymers in multilayer systems. In the first part of this work, different nanokeratin loadings were incorporated into commercial PHA matrices with different hydroxyvalerate content (PHBV3 and PHBV12) by melt compounding. To this end, two different strategies were followed: the traditional method of direct melt blending the additive with the matrix and a preincorporation method in which nanokeratin was electrospun into PHBV3 fibers to generate masterbatches which were then melt mixed with PHBV3 pellets. The incorporation of nanokeratin successfully reduced water vapor and oxygen permeability, achieving a high level of dispersion for 0.5 and

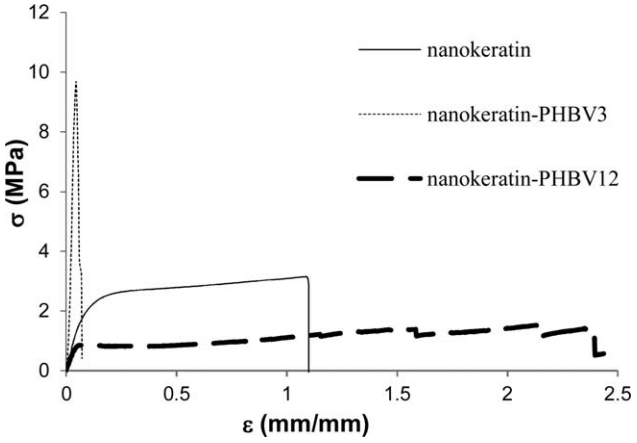

Figure 7. Typical stress–strain curves of the multilayer structures.

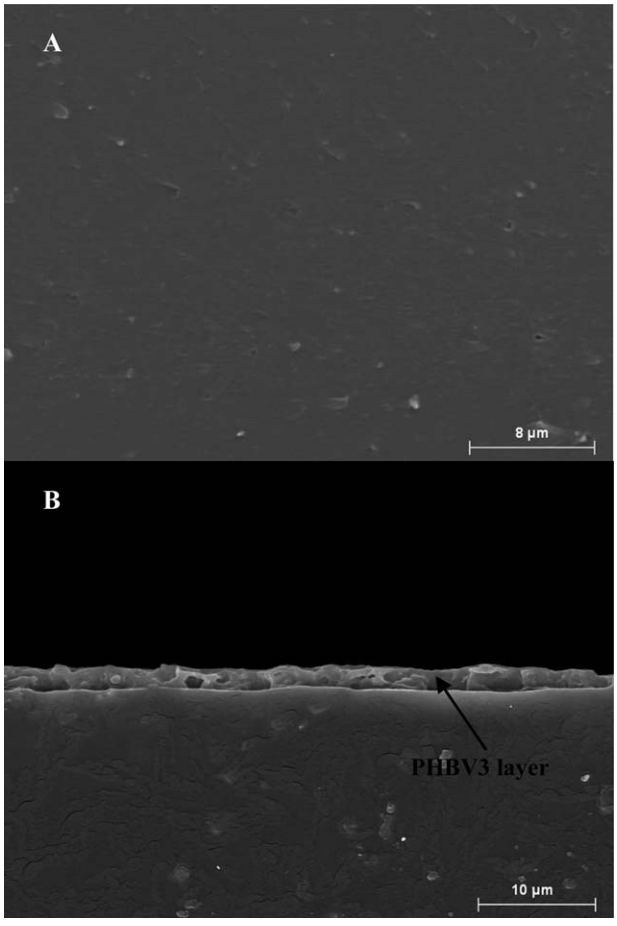

Figure 8. SEM micrograph of (A) the cryofractured section of the pure nanokeratin and (B) the corresponding multilayer system based on nanokeratin (inner layer) and PHBV3 (outer layers).

Table V. Water Vapor Permeability (WVP) and Water Uptake Measured at 100% RH and Estimated Water Diffusivity (D), and Oxygen Permeability O_2P Measured at 80% RH. Mean Value (Standard Deviation)

	WVP (0–75% RH) (kg m s^{-1} m^{-2} Pa^{-1})	Water uptake (%)	D (m^2/s) ($\times 10^{-12}$)	O_2 P (80% RH) (m^3 m m^{-2} s^{-1} Pa^{-1})
Nanokeratin	4.53 (1.15) $e^{-14\ a}$	8.43 (0.07)[a]	1.32	–
Nanokeratin–PHBV3	1.66 (0.21) $e^{-14\ b}$	2.18 (0.06) [b]	1.67	2.54 (0.10) $e^{-18\ a}$
Nanokeratin–PHBV12	2.73 (0.61) $e^{-14\ ab}$	6.68 (0.05) [c]	1.10	16.90 (0.18) $e^{-18\ b}$
Film PHBV3	0.15 (0.07) $e^{-14\ d}$	–	–	0.14 (0.05) $e^{-18\ c}$
Film PHBV12	0.41 (0.03) $e^{-14\ d}$	–	–	0.41 (0.04) $e^{-18\ d}$

[a–e] Different superscripts within the same column indicate significant differences among nanocomposites.

3 wt % loading in PHA matrices with 3 and 12 mol % of hydroxyvalerate, respectively. This resulted in water vapor reductions of up to 63% for both PHA nanocomposites, whereas oxygen permeability improvements depended on the PHA grade. For a given nanokeratin loading, the preincorporation method improved the stretchability of the nanocomposites and they showed reduced water vapor permeability. Interestingly, nanokeratin was more efficient in enhancing barrier properties of PHA nanocomposite films than other nanofillers previously reported. In a subsequent study, an innovative approach was used, involving the coating of the nanokeratin films by electrospun biopolyester fibers homogenized by annealing in order to protect the nanokeratin film from moisture. Coated systems showed a hydrophobic surface (contact angle values>70°). The water vapor permeability of the nanostructured multilayer systems thus obtained dropped by up to *ca* 63% and the oxygen permeability became measurable at high relative humidity and showed a significant barrier effect but lower than that of a pure layer of PHA.

ACKNOWLEDGMENTS

The authors acknowledge the financial support from MINECO (MAT2012–38947-C02-01 project) and the FP7 IP project "ECOBIOCAP". M. J. Fabra is the recipient of a Juan de la Cierva contract from the Spanish Ministry of Economy and Competitivity.

REFERENCES

1. Haugaard, V. K.; Udsen, A. M.; Mortensen, G.; Hoegh, L.; Petersen, K.; Monahan, F. In: Biobased Packaging Materials for the Food Industry Status and Perspectives; Weber C. J., Ed.; A European concerted action, 13, Copenhagen, **2001**.
2. Lagaron, J. M.; Gimenez, E.; Sanchez-Garcia, M. D. In Environmentally compatible food packaging; Chiellini, E., Ed.; Woodhead Publishing Cambridge Ltd., **2008**.
3. Petersen, K.; Nielsen, P. K.; Bertelsen, G.; Lawther, M.; Olsen, M. B.; Nilsson, N. H.; Mortensen, G. *Trend Food Sci. Technol.* **1999**, *10*, 52.
4. Reguera, J.; Lagaron, J. M.; Alonso, M.; Reboto, V.; Calvo, B.; Rodriguez-Cabello, J. C. *Macromolecules* **2003**, *36*, 8470.
5. Malafaya, P. B.; Silva, G. A.; Reis, R. L. *Adv. Drug Deliver. Rev.* **2007**, *59*, 207.
6. Barone, J. R.; Schmidt, W. F.; Liebner, C. F. E. *J. Appl. Polym. Sci.* **2005**, *97*, 1644.
7. Cheng, S.; Lau, K.; Liu, T.; Zhao, Y.; Lam, P. M.; Yansheng, Y. *Compos. Part B Eng.* **2009**, *40*, 650.
8. Tanabe, T.; Okitsu, N.; Tachibana, A.; Yamauchi, K. *Biomaterials* **2002**, *23*, 817.
9. Pardo Ibañez, P.; López-Rubio, A.; Martínez-Sanz, M.; Cabedo, L.; Lagaron, J. M. *J. Appl. Polym. Sci.* **2014**, *131*(4), 39947.
10. Fabra, M. J.; López-Rubio, A.; Lagaron, J. M. *Food Hydrocoll.* **2015**, *44*, 292.
11. Martínez-Sanz, M.; López-Rubio, A.; Villano, M.; Oliveira, C. S. S.; Majone, M.; Reis, M.; Lagaron, J. M. *J. Appl. Polym. Sci.* DOI: 10.1002/app.42486.
12. Schrooyen, P. M. M.; Dijkstra, P. J.; Oberthu, R. C.; Bantjes, A.; Feijen, J. *J. Agric. Food Chem.* **2000**, *48*, 4326.
13. Barham, P. J.; Keller, A.; Otun, E. L.; Holmes, P. A. *J. Mater. Sci.* **1984**, *19*, 2781.
14. ASTM. Standard test methods for water vapor transmission of materials. Standards designations: E96-95. In Annual Book of ASTM Standards. American Society for Testing and Materials: Philadelphia, PA, **2011**; p 406.
15. ASTM D628-10. Standard Test Method for Tensile Properties of Plastics. In: Annual Book of ASTM Standards. American Society for Testing and Materials: Philadelphia, PA.
16. Bras, J.; Viet, D.; Bruzzese, C.; Dufresne, A. *Carbohydr. Polym.* **2011**, *84*, 211.
17. Martínez-Sanz, M.; López-Rubio, A.; Lagaron, J. M. *Biomacromolecules* **2012**, *13*, 3887.
18. Jiang, L.; Morelius, E.; Zhang, J.; Wolcott, M.; Holbery, J. *J. Compos. Mater.* **2008**, *42*, 2629.
19. Ten, E.; Bahr, D. F.; Li, B.; Jiang, L.; Wolcott, M. P. *Ind. Eng. Chem. Res.* **2012**, *51*, 2941.
20. Sanchez-Garcia, M. D.; Lagaron, J. M. *J. Appl. Polym. Sci.* **2010**, *118*, 188.

21. Martínez-Sanz, M.; Vicente, A. A.; Gontard, N.; Lopez-Rubio, A.; Lagaron, J. M. *Cellulose* **2014**, *22*, 535.
22. Modi, S.; Koelling, K.; Vodovotz, Y. *Eur. Polym. J.* **2011**, *47*, 179.
23. Martínez-Sanz, M.; Villano, M.; Oliveira, C.; Albuquerque, M. G. E.; Majone, M.; reis, M.; López-Rubio, A.; Lagaron, J. M. *New Biotechnol.* **2014**, *31*, 364.
24. Fabra, M. J.; López-Rubio, A.; Lagaron, J. M. *Food Hydrocoll.* **2013**, *32*, 106.
25. Sanchez-Garcia, M. D.; Gimenez, E.; Lagaron, J. M. *Carbohydr. Polym.* **2008**, *71*, 235.
26. Sanchez-Garcia, M. D.; Lagaron, J. M. *J. Appl. Polym. Sci.* **2008**, *108*, 2787.
27. Fabra, M. J.; Talens, P.; Chiralt, A. *J. Food Eng.* **2010**, *96*, 356.
28. Jiménez, A.; Fabra, M. J.; Talens, P.; Chiralt, A. *Food Hydrocoll.* **2012**, *26*, 302.
29. Modi, S.; Koelling, k.; Vodovotz, Y. *Macromolecules* **1976**, *9*, 774.